

Electronic Supplementary Information for

A hierarchical carbon foam-hosted Co₂P nanoparticles monolithic electrode for ampere-level and super-durable electrocatalytic hydrogen production

Yaoyao Zhao,^{a,b,c} Zhengguo Zhang,^{*a,b,c} Fang Wang ^{a,b,c} and Shixiong Min ^{*a,b,c}

^a *School of Chemistry and Chemical Engineering, North Minzu University, Yinchuan, 750021, P. R. China. E-mail: sxmin@nun.edu.cn*

^b *Ningxia Key Laboratory of Solar Chemical Conversion Technology, North Minzu University, Yinchuan 750021, P. R. China. E-mail: zhangzhengguo1119@126.com*

^c *Key Laboratory of Chemical Engineering and Technology, State Ethnic Affairs Commission, North Minzu University, Yinchuan, 750021, P. R. China.*

1. Experimental

1.1 Chemicals and materials

All chemicals were of analytical grade and used without further purification. $\text{Co}(\text{NO}_3)_2 \cdot 6\text{H}_2\text{O}$ (99.0%) and KOH (90.0%) were purchased from Shanghai Titan Scientific Co., Ltd. $\text{NaH}_2\text{PO}_2 \cdot \text{H}_2\text{O}$ (AR) was purchased from Shanghai Macklin Biochemical Co., Ltd (Shanghai, China). Commercial Pt/C (20 wt.% Pt) catalyst was purchased from Alfa Aesar (Shanghai, China). PVA sponge were purchased from Yiwu Junman E-commerce Co., Ltd. (Zhejiang, China). All solutions were prepared with ultrapure water (18.2 M Ω cm) obtained from a water purification system (Hitech ECO-S15).

1.2 Preparation of Co@HCF and Co₂P@HCF electrodes

The purchased PVA sponge was first freeze-dried for 24 h, then cut into thin slices (2 cm×2.5 cm×1 cm), and finally soaked into 0.1 M $\text{Co}(\text{NO}_3)_2$ aqueous solution at room temperature for 2 h and freeze-dried for 24 h to obtain Co^{2+} -adsorbed polyvinyl alcohol sponge (Co^{2+} -PS). The Co^{2+} -PS was then pretreated at 260 °C for 6 h in air and carbonized at 1000 °C for 6 h in an Ar atmosphere with a ramping rate of 5 °C min⁻¹ to obtain Co@HCF electrode. The phosphorization of Co@HCF was carried out in a tube furnace where the $\text{NaH}_2\text{PO}_2 \cdot \text{H}_2\text{O}$ (1.8 g) was loaded at the upstream side, and the furnace was heated at 300 °C for 2 h under Ar atmosphere with heating rate of 2 °C min⁻¹. The as-obtained Co₂P@HCF electrode was polished with 2000 grit sandpaper to ~ 1.0 mm, washed in water and ethanol by ultrasonication, and finally dried in vacuum oven at 60 °C.

1.3 Characterization

X-ray diffraction (XRD) patterns were recorded using the Rigaku Smartlab diffractometer with a nickel filtrated Cu K α radiation in the 2 θ range of 5~80° with a

scanning rate of $10^\circ \text{ min}^{-1}$. Scanning electron microscopy (SEM) images were taken with a scanning electron microscope (ZEISS Sigma 500). Transmission electron microscopy (TEM) images were taken with a field emission transmission electron microscope (FEI Talos F200x). The elemental content was determined by inductively coupled plasma-optical emission spectroscopy (ICP-OES) (Agilent 5110). X-ray photoelectron spectroscopy (XPS) measurements were performed on a Thermo Scientific Escalab-250Xi electron spectrometer using an Al $K\alpha$ X-ray source. Raman spectra were collected by using a Horiba Evolution Raman spectrometer with a 532 nm laser as an excitation source. Brunauer-Emmett-Teller (BET) equation at 77 K was determined with Micromeritics ASAP 2460 to calculate the specific surface area of the electrodes. The compression tests were carried out by a single-column system (HZ-1003) at a constant loading speed of 3 mm min^{-1} . The contact angles of the electrodes were evaluated on a JGW-360 A goniometer (China).

1.4 Electrochemical measurements

All electrochemical tests were conducted with a standard three-electrode system at a CorrTest3103 (CorrTest, Wuhan, China) electrochemical workstation. Ag/AgCl (0.5 M H_2SO_4 solution) and saturated Hg/HgO (1.0 M KOH solution) were used as reference electrode, and a graphite rod as the counter electrode, respectively. As-fabricated monolithic electrodes were directly used as working electrode. All potentials were referenced to the reversible hydrogen electrode (RHE) by the equation: $E_{\text{RHE}} = E_{\text{Hg/HgO}} + 0.0591 \text{ pH} + 0.098 \text{ V}$; $E_{\text{RHE}} = E_{\text{Ag/AgCl}} + 0.0591 \text{ pH} + 0.197 \text{ V}$. The polarization curves of HER were measured by linear sweep voltammetry (LSV) at a scan rate of 0.5 mV s^{-1} in 0.5 M H_2SO_4 and 1.0 M KOH solution, respectively. The LSV were corrected by IR compensation. The durability of catalyst was evaluated in 0.5 M H_2SO_4 and 1.0 M KOH solution by chronopotentiometric test. The

electrochemical active surface area (ECSA) was obtained from cyclic voltammetry (CV) from the electrochemical double-layer capacitances (C_{dl}). Electrochemical impedance spectroscopy (EIS) was measured under an AC amplitude of 10 mV with a frequency range of 0.01 Hz to 10 kHz.

1.5 Estimation of active site number and turnover frequency (TOF)

The underpotential deposition (UPD) of Cu has been used to estimate the number of active sites for the electrodes. Briefly, the electrochemical cleaning of the electrodes was performed in a 0.5 M H_2SO_4 +20 mM $CuSO_4$ +60 mM NaCl solution at 1.0 V vs. Ag/AgCl for 180 s, followed by the deposition of Cu at various underpotentials for 120 s in the same solution. A LSV was then performed at 1 mV s^{-1} from the set underpotential to a point at which all the UPD Cu had been removed. The active site number and the corresponding TOFs of the HER in both alkaline and acidic solutions can be estimated from the required charges for copper stripping according to the following equations (2) and (3), respectively:

$$N_A = \frac{Q_{Cu^{2+}}}{2FS} \quad (2)$$

$$TOF(h^{-1}) = \frac{j_i}{zFN_A} \times 3600 \quad (3)$$

where N_A ($mol\ cm^{-2}$) represents the density of active sites, S (cm^2) is the geometric area of the electrode, $Q_{Cu^{2+}}$ (C) is the required charges for UPD stripping, F is the Faradaic constant ($96485\ C\ mol^{-1}$), and j_i is the current density at a certain overpotential potential ($A\ cm^{-2}$).

2. Additional data

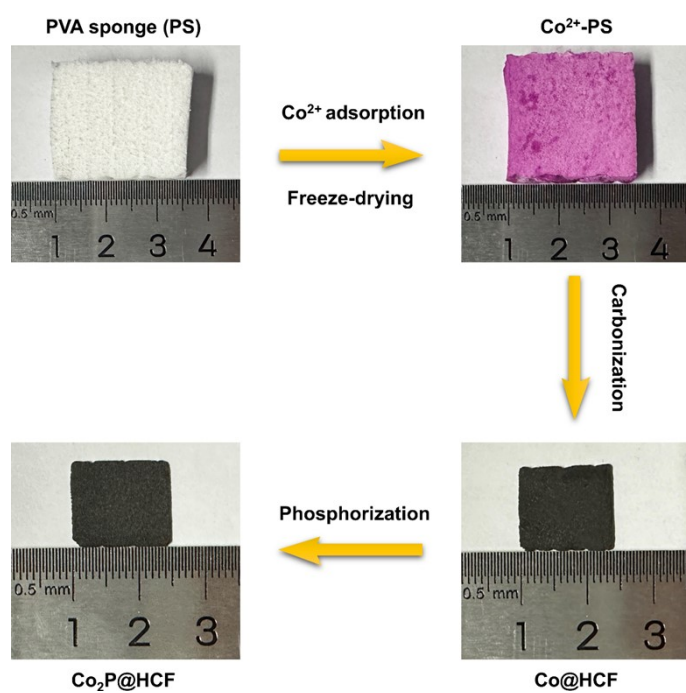


Fig. S1 Schematics of preparation of Co₂P@HCF monolithic electrode.

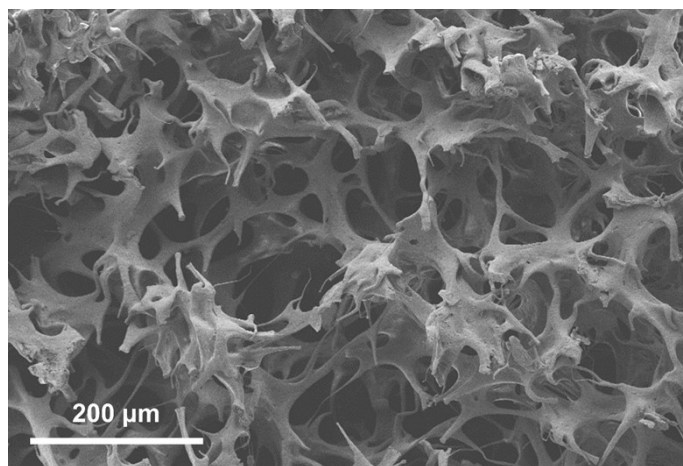


Fig. S2 SEM image of the PS.

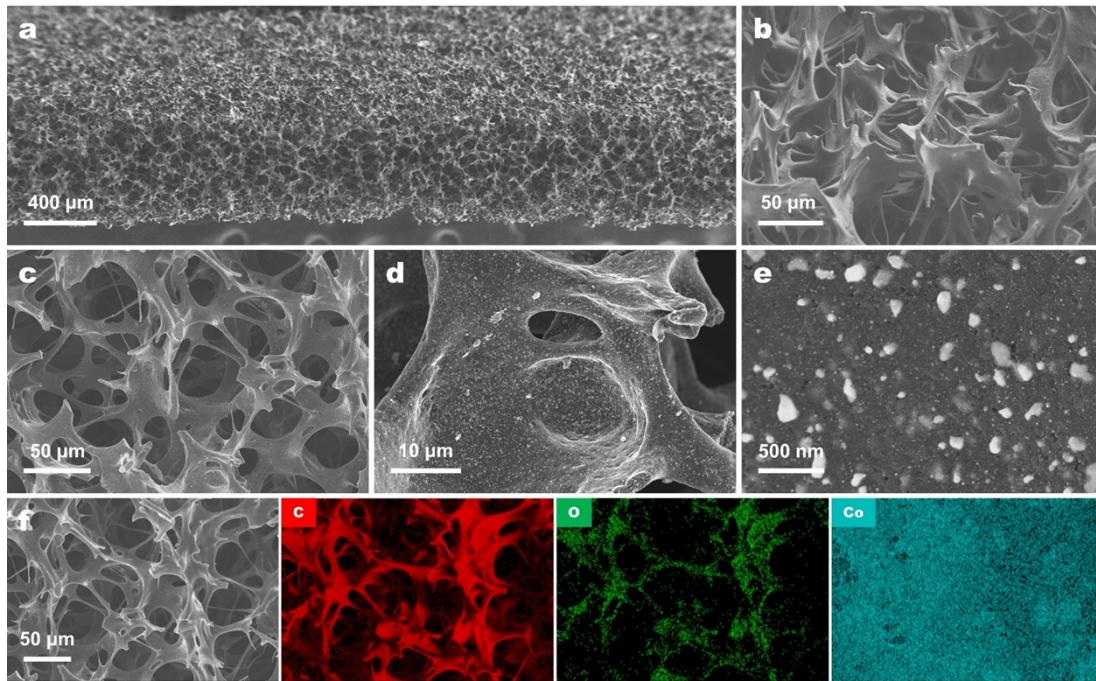


Fig. S3 (a) SEM image showing the overall view of Co@HCF electrode. (b) Top-view, (c) side-view, and (d, e) high-resolution SEM images of Co@HCF electrode. (f) SEM image of Co@HCF electrode and the corresponding EDX mappings.

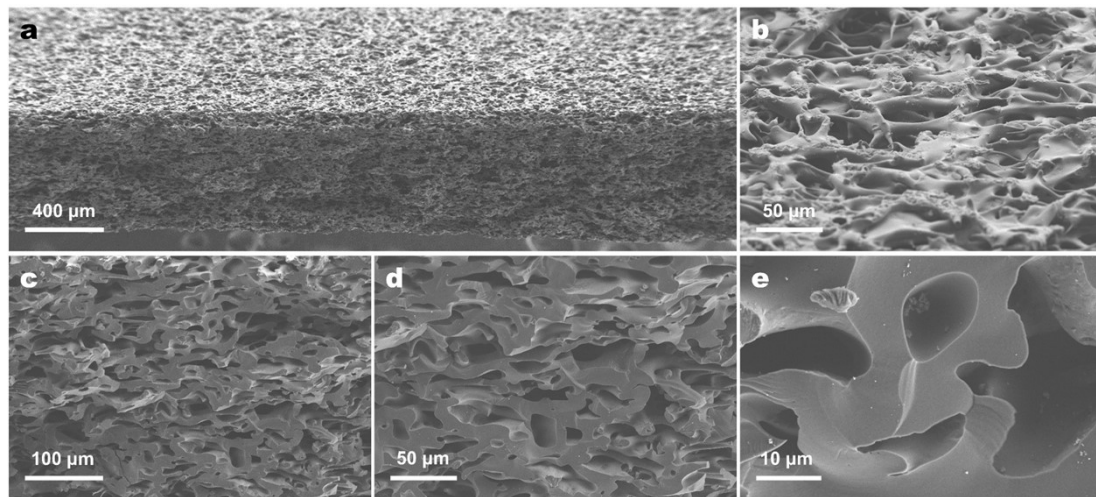


Fig. S4 (a) SEM image showing the overall view of CPS. (b) Top-view, (c, d) side-view, and (e) high-resolution SEM images of CPS electrode.

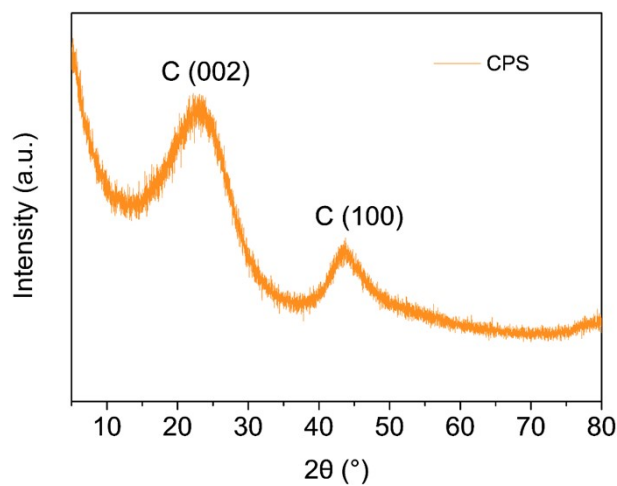


Fig. S5 XRD pattern of the CPS electrode.

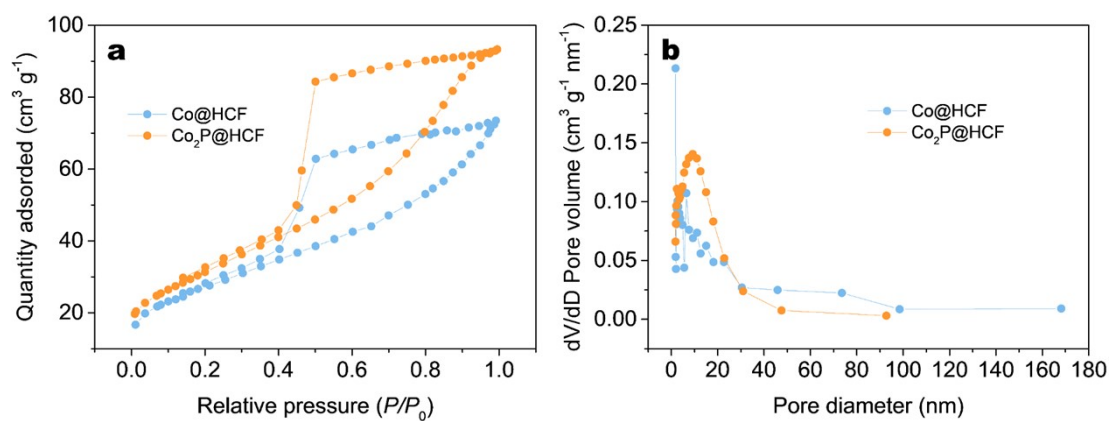


Fig. S6 (a) N_2 adsorption-desorption isotherms and (b) pore size distributions of $Co@HCF$ and $Co_2P@HCF$ electrodes.

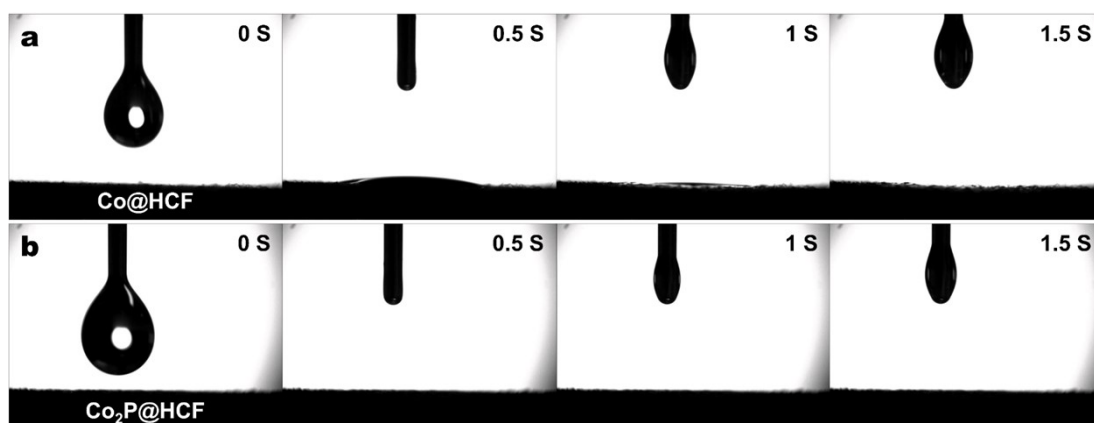


Fig. S7 Electrolyte wettability of (a) $Co@HCF$ and (b) $Co_2P@HCF$ electrodes.

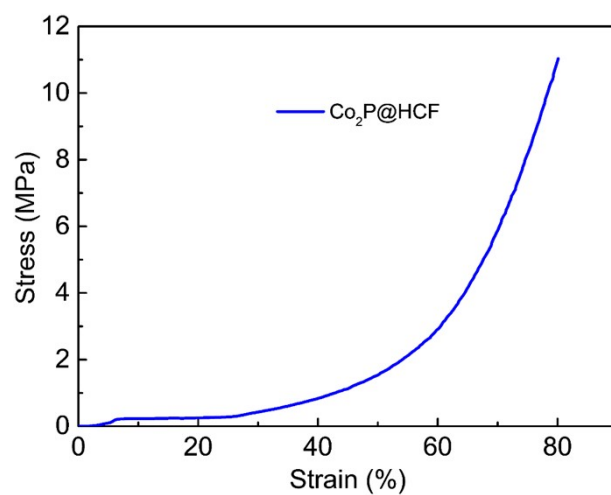


Fig. S8 Compressive stress-strain curve of Co₂P@HCF electrode.

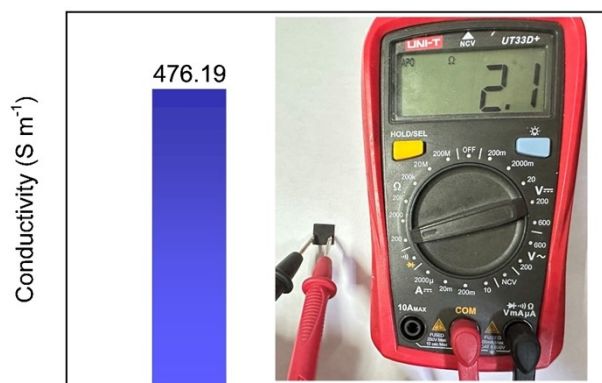


Fig. S9 Electrical conductivity of Co₂P@HCF.

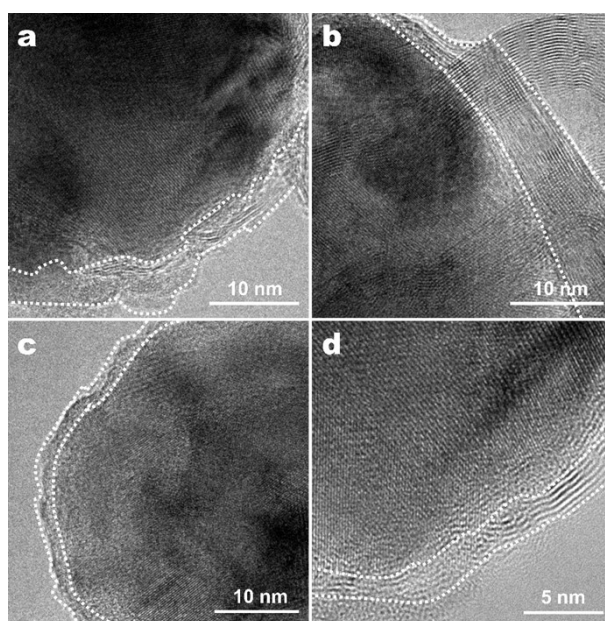


Fig. S10 High-resolution TEM images of Co₂P@HCF electrode.

Table S1 XPS elemental analysis of Co@HCF and Co₂P@HCF electrodes.

Electrode	C (at.%)	O (at.%)	Co (at.%)	P (at.%)
Co@HCF	64.77	28.29	6.94	—
Co ₂ P@HCF	30.91	34.82	13.34	20.93

Table S2 ICP-OES analysis of Co@HCF and Co₂P@HCF electrodes.

Electrode	Co (wt.%)	P (wt.%)	Co/P ratio
Co@HCF	19.44	0	—
Co ₂ P@HCF	20.35	6.88	1.55:1

Table S3 Comparison of electrocatalytic HER performance at high current densities for Co₂P@HCF with other reported electrocatalysts in 1.0 M KOH solution.

Catalyst	Overpotential (mV)	Reference
Co ₂ P@HCF	194.7 mV@500 mA cm ⁻² 218.6 mV@1000 mA cm ⁻²	This work
Ni-W nanosheet	303 mV@500 mA cm ⁻²	[1]
Ni ₂ P/NF	306 mV@1000 mA cm ⁻²	[2]
NiMoO _x /NiMoS	174 mV@500 mA cm ⁻² 236 mV@1000 mA cm ⁻²	[3]
MoS ₂ /Mo ₂ C	220 mV@1000 mA cm ⁻²	[4]
F-Co ₂ P/Fe ₂ P	261 mV@1000 mA cm ⁻²	[5]
A-NiCo LDH/NF	381 mV@1000 mA cm ⁻²	[6]
Ni _x Co _{3-x} S ₄ /Ni ₃ S ₂ /NF	432 mV@500 mA cm ⁻²	[7]
Sn-Ni ₃ S ₂ /NF	570 mV@1000 mA cm ⁻²	[8]

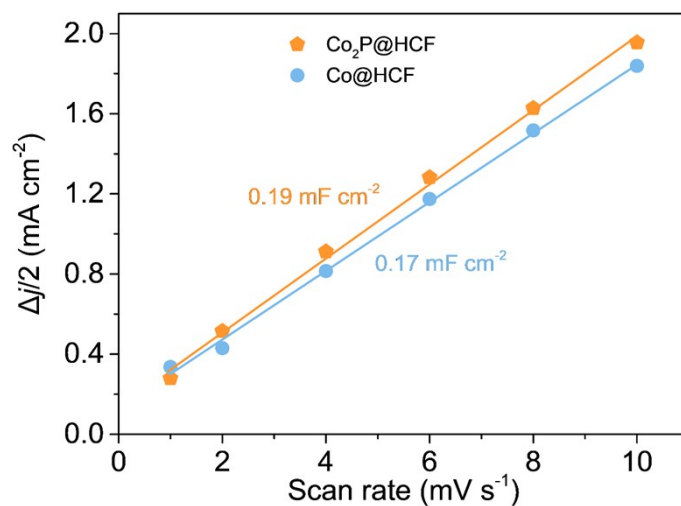


Fig. S11 Electrochemical double-layer capacitive currents of Co@HCF and Co₂P@HCF electrodes in 1.0 M KOH.

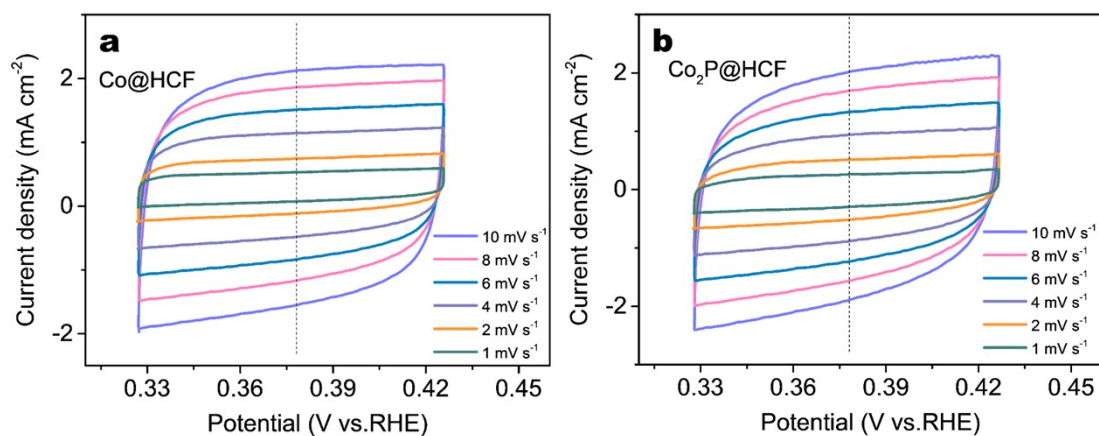


Fig. S12 CV curves of (a) Co@HCF and (b) Co₂P@HCF electrodes at different scan rates: 1-10 mV s⁻¹ in 1.0 M KOH.

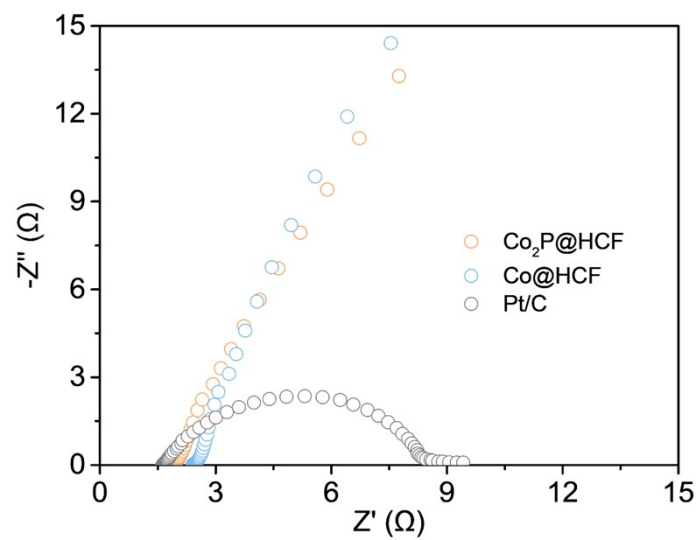


Fig. S13 Nyquist plots of Co₂P@HCF, Co@HCF, and Pt/C electrodes in 1.0 M KOH.

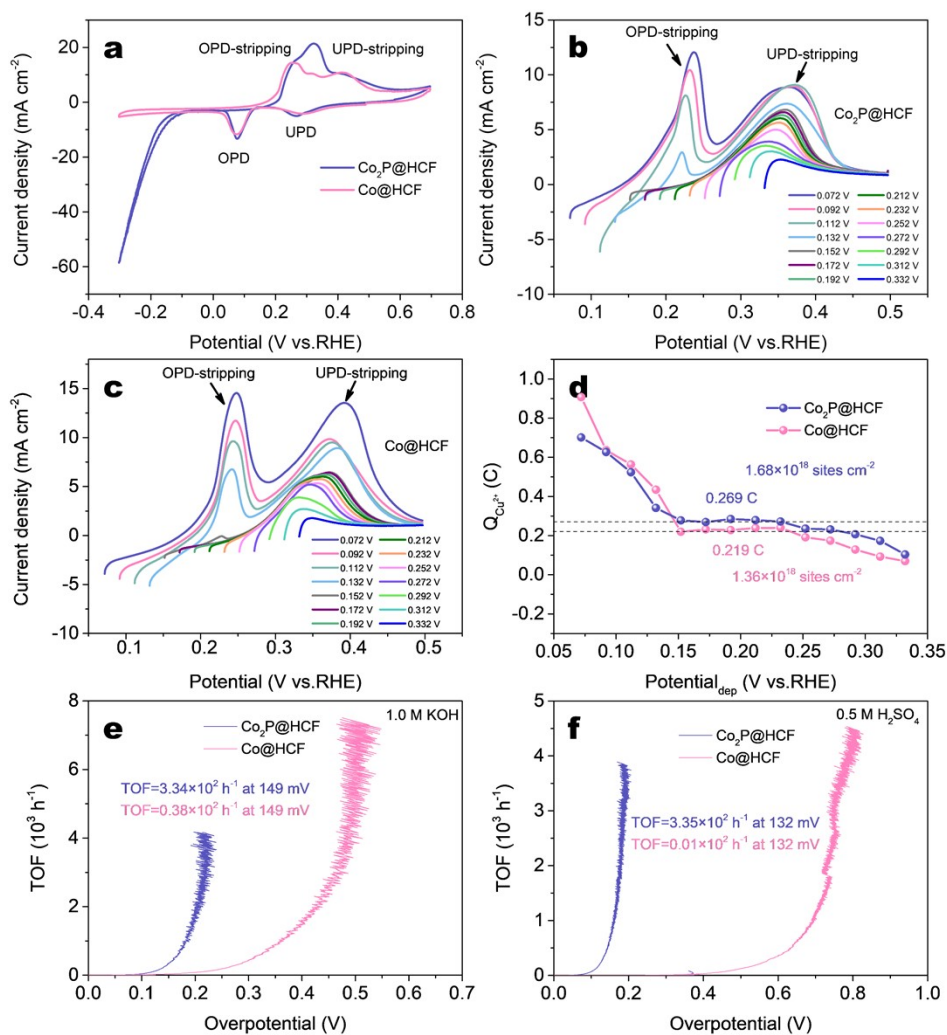


Fig. S14 (a) CV curves for Co₂P@HCF and Co@HCF electrodes in a solution of 0.5 M H₂SO₄+20 mM CuSO₄+60 mM NaCl at a scan rate of 1 mV s⁻¹. LSV curves of (b) Co₂P@HCF and (c) Co@HCF electrodes for the stripping of Cu deposited at different overpotentials from 0.072 to 0.332 V vs. RHE in a 0.5 M H₂SO₄+20 mM CuSO₄+60 mM NaCl solution (scan rate of 1 mV s⁻¹). (d) The charges required to strip the Cu deposited at different underpotentials for Co₂P@HCF and Co@HCF electrodes. The dependences of TOF on overpotential for the HER in (e) alkaline and (f) acidic solutions over the Co₂P@HCF and Co@HCF electrodes.

Table S4 Comparison of electrocatalytic HER performance at high current densities for Co₂P@HCF with other reported electrocatalysts in 0.5 M H₂SO₄ solution.

Catalyst	Overpotential (mV)	Reference
Co ₂ P@HCF	173.0 mV@500 mA cm ⁻² 189.6 mV@1000 mA cm ⁻²	This work
MoS ₂ /CNF	450 mV@1000 mA cm ⁻²	[9]
HC-MoS ₂ /Mo ₂ C	412 mV@1000 mA cm ⁻²	[10]
MoC-Mo ₂ C-690	362 mV@500 mA cm ⁻²	[11]
Co/Se-MoS ₂ -NF	382 mV@1000 mA cm ⁻²	[12]
Ni ₂ P-CuP ₂	600 mV@1000 mA cm ⁻²	[13]
α-MoB ₂	334 mV@1000 mA cm ⁻²	[14]
Ni@NCW-2.0	381 mV@500 mA cm ⁻² 401 mV@1000 mA cm ⁻²	[15]
CoP/Ni ₃ P ₄ /CoP	142 mV@1000 mA cm ⁻²	[16]

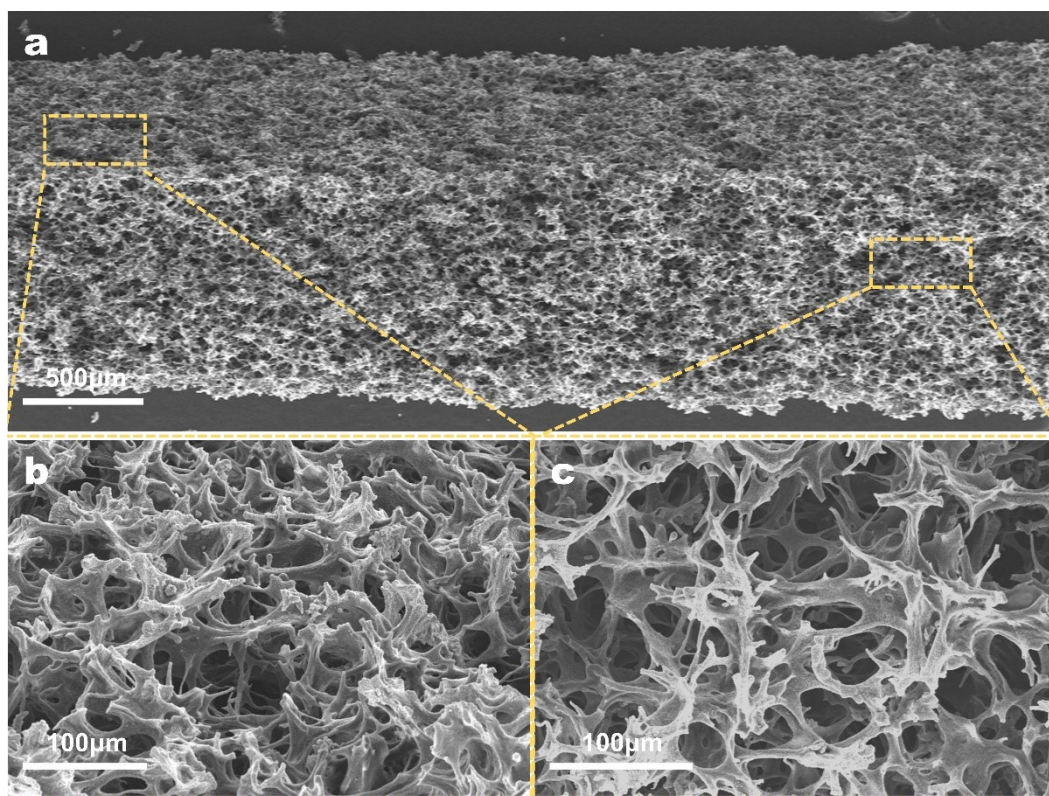


Fig. S15 SEM images of the Co₂P@HCF electrode after long-term HER stability test in 1.0 M KOH solution.

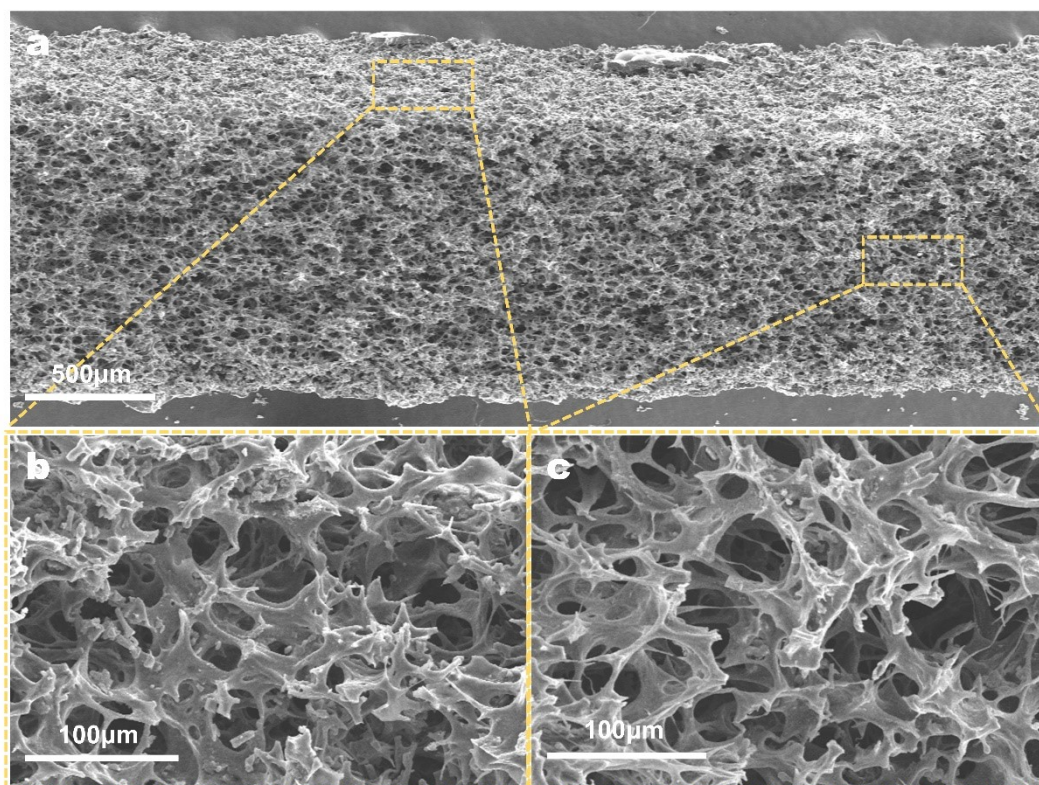


Fig. S16 SEM images of the $\text{Co}_2\text{P@HCF}$ electrode after long-term HER stability test in 0.5 M H_2SO_4 solution.

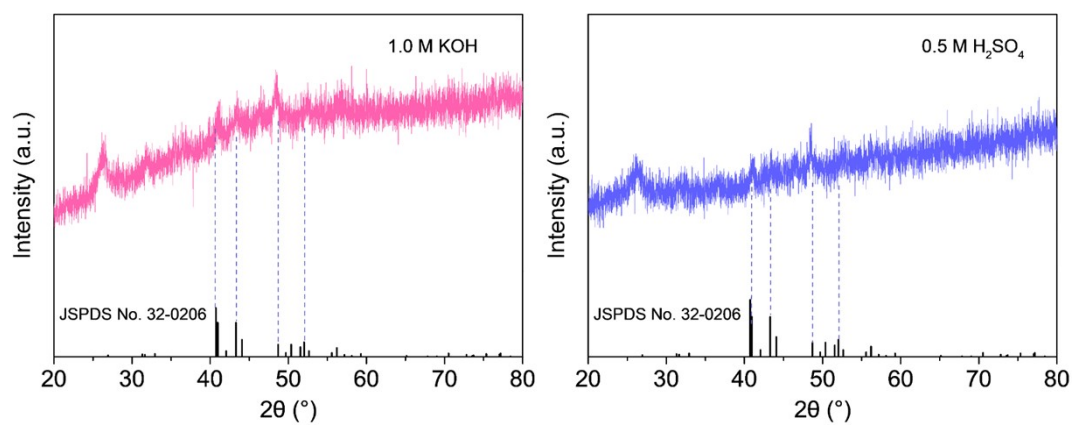


Fig. S17 XRD pattern of the $\text{Co}_2\text{P@HCF}$ electrode after long-term HER stability test.

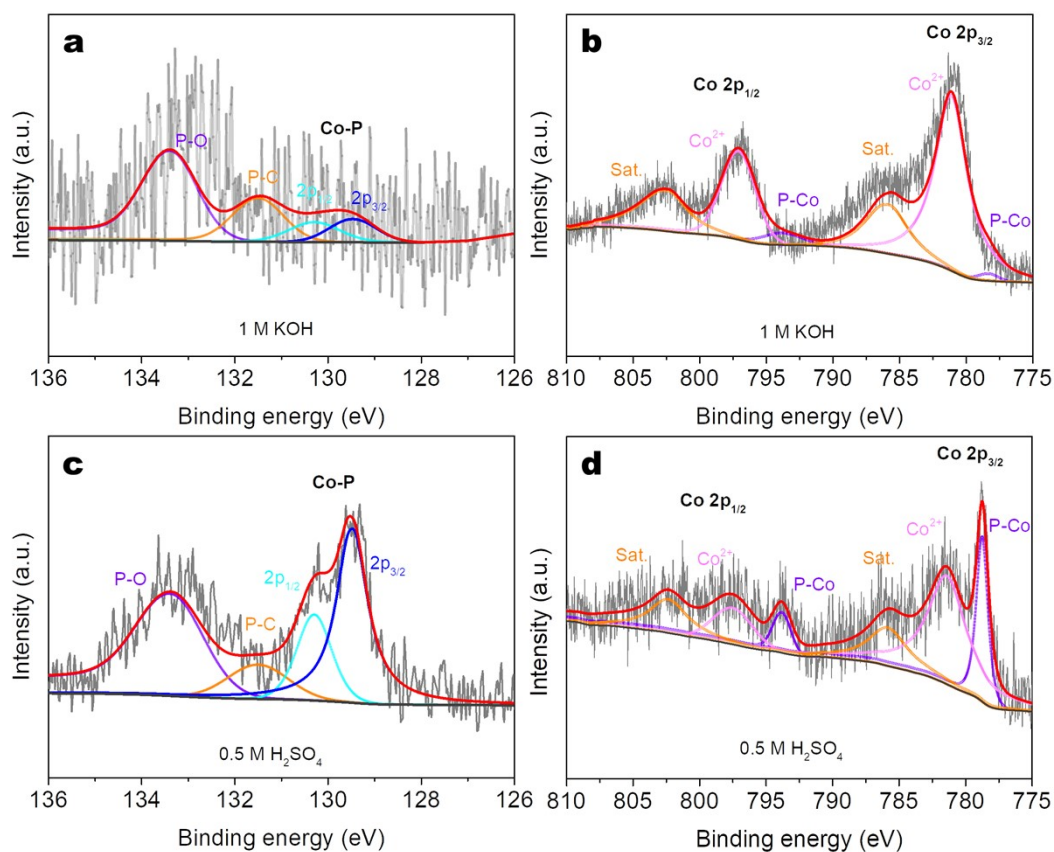


Fig. S18 (a) P 2p and (b) Co 2p XPS spectra of Co₂P@HCF electrode after long-term HER stability test in 1.0 M KOH solution. (c) P 2p and (d) Co 2p XPS spectra of Co₂P@HCF electrode after long-term HER stability test in 0.5 M H₂SO₄ solution.

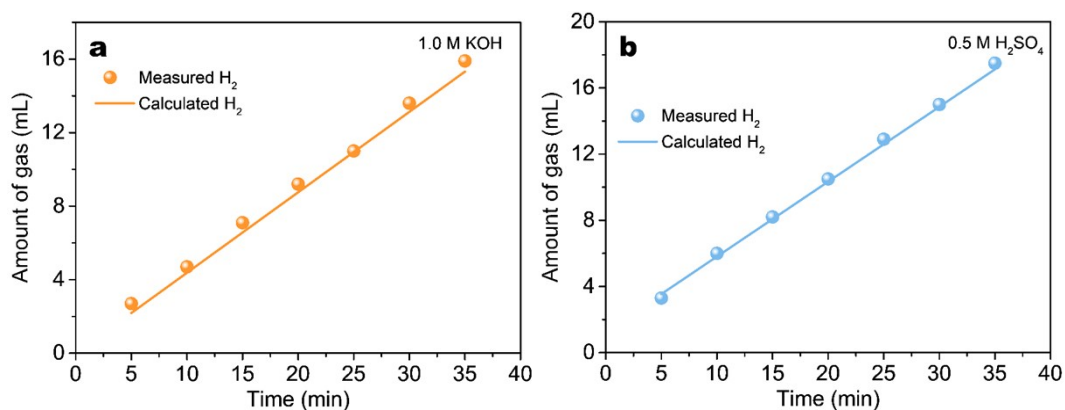


Fig. S19 FEs of Co₂P@HCF for HER in (a) 1.0 M KOH and (b) 0.5 M H₂SO₄ solutions at 50 mA cm⁻².

References

1. H. Wu, L. Kong, Y. Ji, J. Yan, Y. Ding, Y. Li, S.T. Lee and S. Liu, *Adv. Mater. Interfaces*, 2019, **6**, 1900308.
2. X. Yu, Z.-Y. Yu, X.-L. Zhang, Y.-R. Zheng, Y. Duan, Q. Gao, R. Wu, B. Sun, M.-R. Gao, G. Wang and S.-H. Yu, *J. Am. Chem. Soc.*, 2019, **141**, 7537-7543.
3. P. Zhai, Y. Zhang, Y. Wu, J. Gao, B. Zhang, S. Cao, Y. Zhang, Z. Li, L. Sun and J. Hou, *Nat. Commun.*, 2020, **11**, 5462.
4. Y. Luo, L. Tang, U. Khan, Q. Yu, H.-M. Cheng, X. Zou and B. Liu, *Nat. Commun.*, 2019, **10**, 269.
5. X.-Y. Zhang, Y.-R. Zhu, Y. Chen, S.-Y. Dou, X.-Y. Chen, B. Dong, B.-Y. Guo, D.-P. Liu, C.-G. Liu and Y.-M. Chai, *Chem. Eng. J.*, 2020, **399**, 125831.
6. H. Yang, Z. Chen, P. Guo, B. Fei and R. Wu, *Appl. Catal. B*, 2020, **261**, 118240.
7. Y. Wu, Y. Liu, G.-D. Li, X. Zou, X. Lian, D. Wang, L. Sun, T. Asefa and X. Zou, *Nano Energy*, 2017, **35**, 161-170.
8. J. Jian, L. Yuan, H. Qi, X. Sun, L. Zhang, H. Li, H. Yuan and S. Feng, *ACS Appl. Mater. Interfaces*, 2018, **10**, 40568-40576.
9. Z. Zhang, Y. Wang, X. Leng, V.H. Crespi, F. Kang and R. Lv, *ACS Appl. Energy Mater.*, 2018, **1**, 1268-1275.
10. C. Zhang, Y. Luo, J. Tan, Q. Yu, F. Yang, Z. Zhang, L. Yang, H.-M. Cheng and B. Liu, *Nat. Commun.*, 2020, **11**, 3724.
11. W. Liu, X. Wang, F. Wang, K. Du, Z. Zhang, Y. Guo, H. Yin and D. Wang, *Nat. Commun.*, 2021, **12**, 6776.
12. Z. Zheng, L. Yu, M. Gao, X. Chen, W. Zhou, C. Ma, L. Wu, J. Zhu, X. Meng, J. Hu, Y. Tu, S. Wu, J. Mao, Z. Tian and D. Deng, *Nat. Commun.*, 2020, **11**, 3315.

13. S. Riyajuddin, K. Azmi, M. Pahuja, S. Kumar, T. Maruyama, C. Bera and K. Ghosh, *ACS Nano*, 2021, **15**, 5586-5599.
14. Y. Chen, G. Yu, W. Chen, Y. Liu, G.-D. Li, P. Zhu, Q. Tao, Q. Li, J. Liu, X. Shen, H. Li, X. Huang, D. Wang, T. Asefa and X. Zou, *J. Am. Chem. Soc.*, 2017, **139**, 12370-12373.
15. D. Li, H. Cheng, X. Hao, G. Yu, C. Qiu, Y. Xiao, H. Huang, Y. Lu and B. Zhang, *Adv. Mater.*, 2023, **10**, 2304917.
16. I.K. Mishra, H. Zhou, J. Sun, F. Qin, K. Dahal, J. Bao, S. Chen and Z. Ren, *Energy Environ. Sci.*, 2018, **11**, 2246-2252.